

Room temperature ferromagnetism in Mn-doped γ -Ga₂O₃ with spinel structure

Hiroyuki Hayashi,^{a)} Rong Huang, Hidekazu Ikeno, Fumiyasu Oba,
Satoru Yoshioka, and Isao Tanaka^{b)}

Department of Materials Science and Engineering, Kyoto University, Yoshida, Sakyo, Kyoto 606-8501, Japan

Saki Sonoda

Department of Electronics and Information Science, Kyoto Institute of Technology, Goshokaido, Matsugasaki, Sakyo, Kyoto 606-8585, Japan

(Received 28 July 2006; accepted 10 September 2006; published online 30 October 2006)

Mn-doped Ga₂O₃ (7 cation % of Mn) thin film has been grown on *c*-cut sapphire substrate using pulsed-laser deposition technique. Electron diffraction analyses by transmission electron microscopy found that the Mn-doped film shows γ phase with spinel structure, which is different from undoped film showing β phase. No secondary phase can be detected. Combination of Mn-*L*_{2,3} near edge x-ray absorption experiments with first-principles many-electron calculations unambiguously implies that Mn atoms are located at tetrahedrally coordinated Ga sites with a valence of +2. The doped sample shows ferromagnetism up to 350 K. © 2006 American Institute of Physics. [DOI: 10.1063/1.2369541]

Diluted magnetic semiconductors (DMSs) have attracted keen interests since ferromagnetism in In_{1-x}Mn_xAs (Ref. 1) and Ga_{1-x}Mn_xAs (Ref. 2) was reported. However, they are ferromagnetic only at far below the room temperature. In order to increase the Curie temperature, doping of magnetic elements into wide-gap oxides and nitrides has been attempted.^{3,4} Some reported DMS at room temperature by doping of magnetic elements into wide-gap substances. However, their mechanism is still controversial. In order to go beyond the current situation, systematic investigation of more compounds with detailed analyses of local environments of solutes is mandatory. In 2002, successful growth of Mn-doped GaN films showing room temperature ferromagnetism and *p*-type conductivity was reported.⁵ The estimated Curie temperature was 940 K at 5.7% of Mn, which is the highest among DMS ever reported. Recently the ferromagnetic Mn-doped GaN samples have been investigated to find that Mn atoms are substitutionally dissolved into the GaN lattice and they exhibit mixed valences of +2 (majority) and +3 (minority).⁶ Valency control of Mn seems to be an important strategy for the ferromagnetism.

If the underlying mechanism behind the valency control is understood, it should be possible to make a series of DMS in Mn-doped wide-gap compounds. As the first step, we examine Mn-doped gallia, Ga₂O₃ in the present study. Ga₂O₃ is known to show a few polymorphs, i.e., α , β , γ , δ , and ϵ .⁷ They are different not only in their crystal space group but also in the coordination number (CN) of Ga ions. β -Ga₂O₃ is most commonly available monoclinic crystal, which shows the same number of CN=4 and CN=6 sites. γ -Ga₂O₃ shows a defective spinel structure that is analogous to γ -Al₂O₃. It also has both CN=4 and CN=6 sites.

Thin film samples were prepared by a pulsed-laser deposition (PLD) method using an excimer KrF* laser source ($\lambda = 248$ nm, $\tau = 25$ ns, Lambda Physik COMPex205). The laser power was 3×10^4 J m⁻². Al₂O₃ (0001) single crystal was

used for the substrate, which was kept at 773 K and $p_{O_2} = 0.05$ Pa during the deposition. The oxygen pressure was increased after the deposition to 130 Pa and kept during cooling to the room temperature. The 10 Hz laser was irradiated for 10^4 shots, which yielded thin film with 300 nm thickness. PLD targets with/without Mn were fabricated by mixing of commercially available high-purity powder of MnO₂ with Ga₂O₃ powder followed by sintering in air at 1623 K for 3 h. Powder x-ray diffraction (XRD) analyses found that both of targets are composed of a single crystalline phase of β -Ga₂O₃. The concentration of Mn of doped PLD sample was measured by energy dispersive x-ray spectroscopy equipped to a scanning electron microscope and a transmission electron microscope (TEM). Both of them found an identical result, i.e., 7 cation % of Mn. The phases and crystal structure of samples were analyzed by means of XRD and TEM. In order to identify the local states of Mn atoms, Mn-*L*_{2,3} near edge x-ray absorption fine structures (NEXAFS) measurements were carried out at BL11A in KEK-PF, Tsukuba, Japan using total electron yield method. Magnetic properties of PLD samples were measured by superconducting quantum interference device (SQUID) (Quantum design MPMS) from 2 to 350 K.

Undoped and 7 cation % of Mn-doped PLD samples were obtained by the PLD method. Both of them show a single peak in the θ - 2θ XRD profiles as in Fig. 1. The peak position centered at $2\theta = 37.6^\circ$ for the Mn-doped film can be ascribed to $\gamma(222)$ lattice spacing at 37.28° , or that of $\beta(\bar{4}02)$ at 38.40° as in the case of the undoped film. No other crystalline phase can be detected. Figure 2(a) shows a set of selected-area electron-diffraction patterns for the undoped film obtained from two orientations. Corresponding patterns for the Mn-doped film are given in the upper left and right panels of Fig. 2(b). With an incident electron-beam direction parallel to the Al₂O₃ [$2\bar{1}10$], the patterns from the undoped and Mn-doped films are similar in the positions of main spots. Systematic indexing and simulations identify the patterns as either $\beta[102]$ or $\gamma[2\bar{1}\bar{1}]$, which are found to have a

^{a)}Electronic mail: hayashi@cms.mtl.kyoto-u.ac.jp

^{b)}Electronic mail: tanaka@cms.mtl.kyoto-u.ac.jp

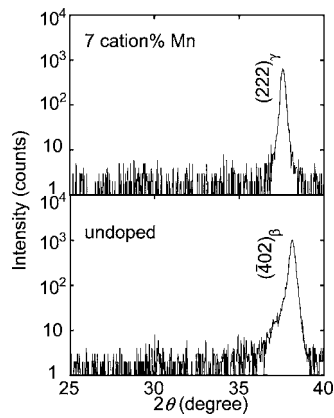


FIG. 1. X-ray diffraction patterns by θ - 2θ method by Cu $K\alpha$ radiation for two PLD samples.

close resemblance despite the difference in crystal structure. The two phases are difficult to differentiate solely from these patterns. In contrast, distinct discrepancies can be found between the two specimens with an orientation parallel to the Al_2O_3 $[10\bar{1}0]$. The patterns for the undoped film can be identified as superposition of three patterns, $[0\bar{1}0]$, $[132]$, and $[1\bar{3}2]$ of the β -phase, arising from more than three grains oriented in respective directions in the selected area. The $[102]$ and $[0\bar{1}0]$ directions are perpendicular to each other. The $[102]$ and $[132]$ directions and the $[102]$ and $[1\bar{3}2]$ directions make an angle of 31.8° , which is close to the angle between the Al_2O_3 $[2\bar{1}\bar{1}0]$ and $[10\bar{1}0]$, 30° . The diffraction patterns with two incident-beam directions correspond to an orientation relationship of β - Ga_2O_3 $(\bar{2}01)\parallel\text{Al}_2\text{O}_3$ (0001) and β - Ga_2O_3 $[102]\parallel\text{Al}_2\text{O}_3$ $[2\bar{1}\bar{1}0]$ or β - Ga_2O_3 $[\bar{1}0\bar{2}]\parallel\text{Al}_2\text{O}_3$ $[2\bar{1}\bar{1}0]$. While no previous reports on the in-plane orientation relationship can be found for this system, the out-of-plane relationship is consistent with the present and previously reported XRD results.⁸ Because of threefold symmetry of the Al_2O_3 (0001) , the above relationship involves three kinds of equivalent in-plane orientations of β - Ga_2O_3 grains. The three

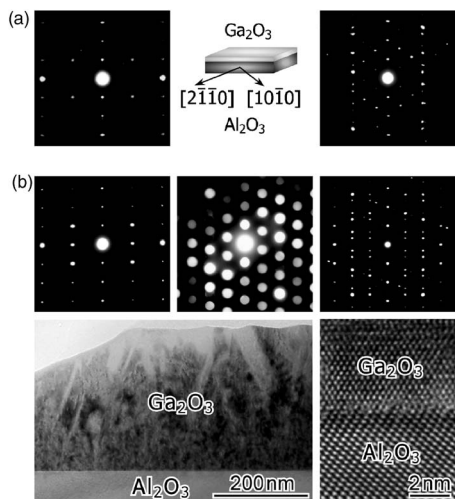


FIG. 2. (a) Selected-area electron-diffraction patterns for an undoped β - Ga_2O_3 film obtained from orientations parallel to the Al_2O_3 $[2\bar{1}\bar{1}0]$ (left) and $[10\bar{1}0]$ (right). (b) Corresponding patterns for a Mn-doped film (upper left and right), alongside a microdiffraction pattern (upper middle), and a bright-field and a high-resolution image (lower).

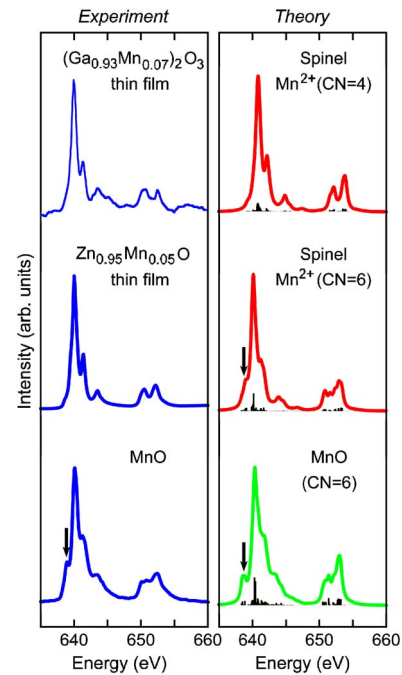


FIG. 3. (Color online) (Left) Experimental Mn- $L_{2,3}$ NEXAFS of the present Mn-doped Ga_2O_3 film in comparison to Mn-doped ZnO^6 and MnO^9 . (Right) Theoretical Mn- $L_{2,3}$ NEXAFS for Mn (CN=4) and Mn (CN=6) in Ga_2O_3 and MnO (CN=6). Thin bars with theoretical spectra show many-electron eigenvalues and corresponding oscillator strengths. The arrows indicate the shoulder peak that is a signature of CN=6.

orientations are recognized in the second diffraction pattern.

The pattern for the Mn-doped specimen is identified as a superposition of the $[10\bar{1}]$ and $[\bar{1}01]$ of γ - Ga_2O_3 . This is supported by an extensive microdiffraction analysis. Either $[10\bar{1}]$ or $[\bar{1}01]$ pattern has been solely obtained from each grain, as recognized in the upper middle panel of Fig. 2(b). The electron and x-ray diffraction analyses can draw a consistent conclusion that Mn-doped γ - Ga_2O_3 is epitaxially grown on the Al_2O_3 (0001) with an orientation relationship of γ - Ga_2O_3 $(111)\parallel\text{Al}_2\text{O}_3$ (0001) and γ - Ga_2O_3 $[2\bar{1}\bar{1}]\parallel\text{Al}_2\text{O}_3$ $[2\bar{1}\bar{1}0]$ or γ - Ga_2O_3 $[2\bar{1}1]\parallel\text{Al}_2\text{O}_3$ $[2\bar{1}\bar{1}0]$. The two kinds of in-plane orientations are connected by inversion symmetry. In the bright-field image shown in the lower left panel, some $\{111\}$ twins can be recognized as linear features making angles of about 70° with the γ - Ga_2O_3 $(111)/\text{Al}_2\text{O}_3$ (0001) interface, corresponding to the angle of 70.5° between $\{111\}$ planes. They are inclined toward left or right, which also indicates the coexistence of grains in the above two orientations. The high-resolution image shows a direct contact of the γ - Ga_2O_3 and Al_2O_3 crystals at the interface without any precipitation. No other phases have been found in the film either.

Figure 3 shows experimental Mn- $L_{2,3}$ NEXAFS of the Mn-doped PLD film. It is compared with reference spectra from $\text{Zn}_{1-x}\text{Mn}_x\text{O}$ ($x=0.05$) (Ref. 6) and MnO .⁹ The peak position of the present sample is the same as those of reference samples, implying that Mn^{2+} is dominant. It is interesting that a shoulder peak at the left-hand side of the L_3 spectrum as indicated by an arrow in the spectrum of MnO is absent in both $\text{Zn}_{1-x}\text{Mn}_x\text{O}$ and the present sample. Mn in the $\text{Zn}_{1-x}\text{Mn}_x\text{O}$ sample was identified to be substitutional at Zn site, showing CN of 4.⁶ This is in contrast to MnO with rocksalt structure with CN=6. The experimental spectrum of

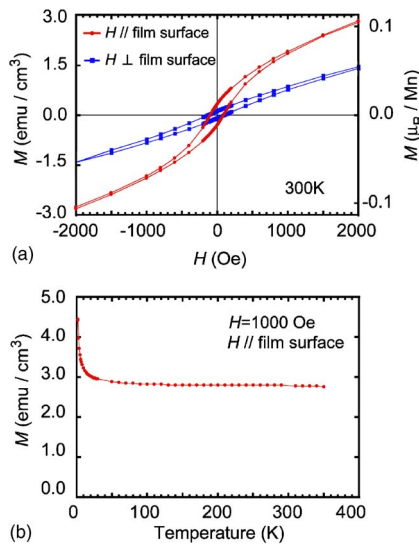


FIG. 4. (Color online) (a) Dependence of magnetization (M) on the magnetic field (H) at 300 K. (b) Temperature dependence of the magnetization at 1 kOe measured in a heating run.

the present PLD film is therefore suggestive of Mn^{2+} with $\text{CN}=4$. In order to confirm the idea, theoretical calculations of the $\text{Mn-L}_{2,3}$ spectrum have been made. A first-principles calculation using density functional theory (DFT) and configuration interaction (CI) scheme has been employed. Details of the DFT-CI computational method are described elsewhere.¹⁰ Computations for the $\text{Mn-L}_{2,3}$ NEXAFS were made for two clusters, i.e., MnO_4^{6-} and MnO_6^{10-} , which correspond to Mn^{2+} with $\text{CN}=4$ and $\text{CN}=6$, respectively. Their atomic positions were taken from MnGa_2O_4 spinel structures that were optimized by a first-principles projector augmented wave method¹¹ using VASP code.^{12–14} A normal spinel structure has all Mn^{2+} at the $\text{CN}=4$ site, which was used for the MnO_4^{6-} model. One of Mn in the 56-atoms supercell was exchanged with a Ga atom in order to make the atomic configuration of the MnO_6^{10-} model. As can be found by the comparison between theoretical and experimental spectra, Mn^{2+} in the spinel Ga_2O_3 is most likely present at the $\text{CN}=4$ site. This is quite natural, since MnGa_2O_4 is known to prefer a normal spinel structure.¹⁵

Figure 4(a) shows the magnetization behavior (M - H curve) of 7 cation % of Mn-doped PLD film at 300 K. The magnetic field was applied parallel or perpendicular to the film. Antimagnetic contribution from the sapphire substrate was subtracted. The magnetization became 8.6 emu/cm³ at 10 kOe when the magnetic field is parallel to the film, which corresponds to 0.42 μ_B /Mn. Figure 4(b) shows the temperature dependence of the magnetization M at 1 kOe, i.e., M - T curve, measured in a heating run after magnetization of the sample at 2 K and 50 kOe. These results are clearly indicative of ferromagnetism up to temperatures higher than 350 K. Origin of the anisotropy in the magnetization is not clear at the moment. The presence of some strain in the film may play a role. The anisotropic behavior cannot be explained by the presence of randomly oriented ferromagnetic particles, which again indicates the intrinsic diluted ferromagnetic nature of γ - $(\text{Ga}_{1-x}\text{Mn}_x)_2\text{O}_3$. Similar behavior has been found for $\text{Ga}_{1-x}\text{Mn}_x\text{N}$.¹⁶ The steep increase in the magnetization at temperatures lower than 30 K has also been observed in $\text{Ga}_{1-x}\text{Mn}_x\text{N}$. A possible interpretation for the increase is the presence of paramagnetic components in the

sample that can contribute for additional magnetization at the low temperatures.

Finally, mechanism behind the ferromagnetism is briefly discussed. MnGa_2O_4 is known to be antiferromagnetic with Néel temperature of 33 K.¹⁵ Since Mn^{2+} ions in MnGa_2O_4 prefer to occupy the $\text{CN}=4$ sites, the coupling among tetrahedrally coordinated Mn^{2+} in spinel structure should be weakly antiferromagnetic in the absence of other mechanisms. The present γ - $(\text{Ga}_{1-x}\text{Mn}_x)_2\text{O}_3$ exhibits some similarity and difference with the ferromagnetic $\text{Ga}_{1-x}\text{Mn}_x\text{N}$ as reported in Ref. 6. In both systems, Mn is predominantly 2+ and located at Ga site of $\text{CN}=4$. Difference between two systems is twofold. Approximately 15% of Mn in $\text{Ga}_{1-x}\text{Mn}_x\text{N}$ is Mn^{3+} , whereas Mn^{3+} is less than the detection limit (a few percent) by the $\text{Mn-L}_{2,3}$ NEXAFS in the present γ - $(\text{Ga}_{1-x}\text{Mn}_x)_2\text{O}_3$. At the same time, $\text{Ga}_{1-x}\text{Mn}_x\text{N}$ shows clear p -type conductivity whereas the electric resistivity of the present γ - $(\text{Ga}_{1-x}\text{Mn}_x)_2\text{O}_3$ is quite high. Assuming that holes in the midgap Mn band, which are associated with the presence of minor Mn^{3+} , act as carriers of p -type conductivity, the electrical properties of two systems can be consistently explained by a single mechanism. Ferromagnetism in γ - $(\text{Ga}_{1-x}\text{Mn}_x)_2\text{O}_3$ may be mediated by smaller amount of holes as compared to $\text{Ga}_{1-x}\text{Mn}_x\text{N}$. More experimental works are being contemplated to improve the model. Spinel structure has a great advantage to make further investigations since properties can be manipulated by doping into two cationic sites with different CNs.

This work was supported by three projects by Japanese Ministry of Education, Culture, Sports, Science and Technology (MEXT). They are the computational materials science unit in Kyoto University, the Grant-in-Aid for Scientific Research (A), and the 21st Century COE program. The NEXAFS experiments at KEK-PF were made under the Proposal No. 2005G212. SQUID measurements were made at Low Temperature Center in Osaka University.

¹H. Munekata, H. Ohno, S. von Molnar, A. Segmüller, L. L. Chang, and L. Esaki, Phys. Rev. Lett. **63**, 1849 (1989).

²H. Ohno, A. Shen, F. Matsukura, A. Oiwa, A. Endo, S. Katsumoto, and Y. Iye, Appl. Phys. Lett. **69**, 363 (1996).

³Y. Matsumoto, M. Murakami, T. Shono, T. Hasegawa, T. Fukumura, M. Kawasaki, P. Ahmet, T. Chikyow, S. Koshihara, and H. Koinuma, Science **291**, 854 (2001).

⁴P. Sharma, A. Gupta, K. V. Rao, F. J. Owens, R. Sharma, R. Ahuja, J. M. Osorio Guillen, B. Johansson, and G. A. Gehring, Nat. Mater. **2**, 673 (2003).

⁵S. Sonoda, S. Shimizu, T. Sasaki, Y. Yamamoto, and H. Hori, J. Cryst. Growth **237**, 1358 (2002).

⁶S. Sonoda, I. Tanaka, H. Ikeno, T. Yamamoto, F. Oba, T. Araki, Y. Yamamoto, K. Suga, Y. Nanishi, Y. Akasaka, K. Kindo, and H. Hori, J. Phys.: Condens. Matter **18**, 4615 (2006).

⁷R. Roy, V. G. Hill, and E. F. Osborn, J. Am. Chem. Soc. **74**, 719 (1952).

⁸M. Orita, H. Hiramatsu, H. Ohta, M. Hirano, and H. Hosono, Thin Solid Films **411**, 134 (2002).

⁹B. Gilbert, B. H. Frazer, A. Belz, P. G. Conrad, K. H. Neilson, D. Haskel, J. C. Lang, G. Srajer, and G. De Stasio, J. Phys. Chem. A **107**, 2839 (2003).

¹⁰H. Ikeno, I. Tanaka, Y. Koyama, T. Mizogushi, and K. Ogasawara, Phys. Rev. B **72**, 075123 (2005).

¹¹P. E. Blöchl, Phys. Rev. B **50**, 17953 (1994).

¹²G. Kresse and J. Hafner, Phys. Rev. B **48**, 13115 (1993).

¹³G. Kresse and J. Furthmüller, Phys. Rev. B **54**, 11169 (1996).

¹⁴G. Kresse and J. Furthmüller, Comput. Mater. Sci. **6**, 15 (1996).

¹⁵B. Boucher, A. G. Herpin, and A. Oles, J. Appl. Phys. **37**, 960 (1966).

¹⁶T. Sasaki, S. Sonoda, Y. Yamamoto, K. Suga, S. Shimizu, K. Kindo, and H. Hori, J. Appl. Phys. **91**, 7911 (2002).